

# Microstructure and Microwave Absorption Properties of Flame Sprayed Ceramic Coatings

Gagan Deep Aul<sup>1</sup>, Vikas Chawla<sup>2</sup>, Santosh K Vishvakarma<sup>3</sup>

<sup>1</sup>Research Scholar, IKGPTU, Jalandhar, Punjab, (India)

<sup>2</sup>Professor, Mechanical Engineering, IKGPTU, Jalandhar, Punjab, (India)

<sup>3</sup>Associate Professor, Electrical Engineering, IIT, Indore (India)

## ABSTRACT

In this research work, airplane grade aluminum alloy substrate was coated by  $Al_2O_3/TiO_2$  ceramic coatings in two different compositions as 50:50 and 87:13 using Flame spraying technique. The surface & cross-sectional morphological characterizations of the  $Al_2O_3/TiO_2$  powders and coatings were performed by scanning electron microscopy (SEM). The microwave absorbing properties of coatings were experimentally investigated using vector network analyzer in the frequency range from 8.2 to 12.4 GHz (X-band). The reflection loss values of  $Al_2O_3/TiO_2$  coatings in 50:50 composition exceeding 10 dB (larger than 90% absorption) was achieved in the frequency range 9.28GHz to 9.82GHz with maximum reflection loss of -11.936dB at 9.53 GHz. It is observed that 87:13 composition of the ceramics  $Al_2O_3/TiO_2$ , gives more than 90% absorption in the frequency range 9.32GHz to 10.21 GHz with a reflection loss peak of -13.6 GHz at 9.683GHz.

**Keywords :** Radar Absorbing Material, Flame Spray, Coatings.

## 1. INTRODUCTION

Due to rapid advancements in the stealth technology, the RAM demands to be thin, lightweight and should be able to possess good reflection loss in the broader range of frequencies. Till today it is a thought-provoking task to develop a thin broadband absorber with improved reflection loss because of stronger trade-off in thickness and bandwidth. Research in development of electromagnetic absorbing coatings /materials gets widespread publicity as its requirement in stealth, EM interference shielding and many more [3-7].

When an EM wave front impinges on a body, part of the energy associated with the wave could get absorbed depending upon the nature of the surface. The rest of the incident energy can then be accounted for, by the phenomena of reflection, diffraction and even refraction, broadly categorized as a scattering phenomenon. The energy reflected back towards the source is called backscattering or Radar Cross Section (RCS). It has been tacitly assumed here that the radar, which is the source of radiation also acts as the receiver; this is referred to as monostatic radar and radar cross section associated with it known as monostatic RCS.

The detectability of target, of which the radar cross section (RCS) is a measure, depends on its external features and EM properties. Detectability can therefore be decreased (stealth) by reducing the RCS of the target [1] From EM prospective, this requires examining the shape of the aerospace body or the other target (which is to be undetected by radar) and the same is to be acceptable to the design engineers of the target that is a big issue as it affects the aerodynamics or related design properties of the target. In such a situation the stealth might rely on

the optimal design acceptable to all concerned engineers.

The Radar signal strength, scattered from a target, determines its detectability, this pertains to RCS that frequently ought to be reduced. The maximum detectable range,  $R_{max}$  [1] for radar is determined by its minimum detectable signal strength  $P_{min}$ :

$$R_{max} = \left[ \frac{P_s G_s^2 \lambda^2 \sigma}{P_{min} (4\pi)^3} \right]^{1/4} \quad (1)$$

Where,  $P_s$ ,  $G_s$ ,  $\lambda$ , and  $\sigma$  are source radar power, transmitting antenna gain, wavelength and target cross section respectively. It is apparent from the equation that the cross section of the target is the only parameter affecting the range; it should be reduced to enhance the survivability of the target. Radar cross section may also be defined with respect to the events on the surface of the scatterer as the ratio of the power scattered to the incident on per unit area of the scatterer:

$$\sigma = \lim_{R \rightarrow \infty} 4\pi R^2 \frac{P_{sc}}{P_{in}} \quad (2)$$

Since the power is related to field, hence eq. (2) can be written as

$$\sigma = \lim_{R \rightarrow \infty} 4\pi R^2 \left| \frac{E_{sc}}{E_{in}} \right|^2 \quad (3)$$

Above equation holds definition, even if the target is a dielectric one, where the backscatter can be reduced due to absorption and even forward scattering. RCS reduction is in fact important for both military and civilian applications. For the military RCSR of such targets as aircraft & missiles in the hostile territory is an important consideration. Similarly making aircrafts hangars near air traffic control radar less reflective is a civilian application. RCS reduction techniques can be broadly classified into four categories viz. shaping, active loading, discrete or passive loading and distributive loading. Shaping involves modification of the external features of the target although it is the excellent method but it has number of issues related like it should be integrated in the system design stage and may not be acceptable to the manufacturer related to other prospective.

The methods employing active & passive elements at selected points where reflections are maximized on the target reduce the overall RCS by phase cancellation. In passive loading technique, special configurations such as resistive sheets are placed over the scattering centers to modify the surface impedance in order to cancel the reflections. In active cancellation, active devices are employed to sense the incident radar waves and to send out signals to cancel the echoes from these points. But these are narrow band width methods and rarely used in actual practices. The distributive loading technique essentially consists of covering the scatter with suitable materials called radar absorbing material (RAM). The RCS is achieved by both absorption and redirection of EM energy. RAM are essentially materials characterized by large values of imaginary part of the permittivity or permeability. The ratio of the imaginary to the real parts of these EM parameters is known as tangent loss. The corresponding materials are identified as the dielectric RAM or magnetic RAM. The mechanism of reduction in the back scatter is thus partly due to scattering in the forward direction through the material and significant absorption of EM waves as it propagates through the coating. Such coatings result in changes in the polarization of the scattered waves which one attributes to the complex nature of propagation of EM waves within RAM coating. The distributive coating is a versatile and universal technique for RCSR as it can be applied at the

stage of production of the target without any modifications in the design or even in the course of retrofitting for upgrading the capabilities of the targets [1].

The above discussion have implicitly assumed and emphasized the perfectly conducting nature of the surface. However should the structure be of dielectric type, the surface EM properties of the scatterer are drastically different? In such a situation the incident EM wave tend to propagate through the surface in the forward scattering direction. Furthermore, EM waves while propagating through the surface also get partially absorbed in the material media, thereby effecting the back scatter RCS.

Alumina is one of the most cost effective and widely used materials in the family of engineering ceramics. Some publications have pointed out the potential of  $Al_2O_3$  and  $TiO_2$  of thermally sprayed coatings for diverse applications [8]. However scarce information is found in literature about the optimum composition of these coatings regarding their absorption capabilities and about the influence of the powder and phase composition on the functionality of the coatings. In this study  $Al_2O_3/TiO_2$  coatings systems were developed using flame spray for radar absorption applications.

## 2. EXPERIMENTAL

### 2.1 SUBSTRATE

Airplane grade material, an aluminum alloy 7075 [9-10] purchased from special metals, Mumbai, India was used as substrate for flame spray coatings. To provide improved strength, corrosion resistance and/or general weldability, aluminum can be alloyed with a number of different elements, both primary and secondary, the primary elements that alloy with aluminum are copper, silicon, manganese, magnesium and zinc. Zinc (7075) added to aluminum with magnesium and copper produces the highest strength heat treatable aluminum alloy. It is primarily used in the aircraft industry [9-10].

The microwave absorption properties effected due to two different compositions  $Al_2O_3/TiO_2$  as 87:13 and 50:50, which are coded as Sample 1 and Sample 2 respectively throughout the study, has been studied. These ceramic powders were arranged from MEC, Jodhpur, India.

### 2.2 FABRICATION

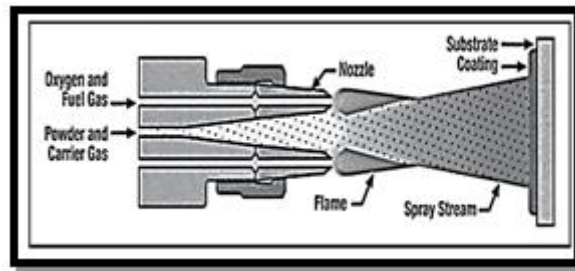
The aluminum alloy 7075 sheet was cut into small samples as 25mm x 19mm x 3.5mm and 23mm x 17mm x 3.5mm [11-12] for coating characterization and electrical properties testing using sheet metal shearing from Sohan industry, Jalandhar. Oxide ceramics commercial feeding-powders were obtained from MEC, Jodhpur, India. The commercial powder characteristics are summarized in Table 1.

Table 1 :  $Al_2O_3-TiO_2$  Commercial Powders Characteristics

Powder Type	Composition	Particle Size
HC Starck $Al_2O_3: TiO_2$	87:13	-45/+15 $\mu$ m
HC Starck $Al_2O_3: TiO_2$	50:50	-45/+15 $\mu$ m

Flame spraying is a very flexible and cost effecting coating process which allows the processing of almost any material [13]. Powder flame spraying, a thermal spray process, coating is achieved by feeding powder through the center bore of a nozzle where it melts and is carried by the escaping oxy-fuel gases to the work

piece Fig. 1.



**Fig. 1: schematic flame spray [2]**

Table 2 : Grit Blasting Details

Grit	20 mesh size virgin Brown Alumina
Blasting	2-5 Kg/sq.cm
Air Pressure	
Surface Roughness	6-10 Ra $\mu$ m
Working Distance	5-6"
Blasting Angle	90 <sup>0</sup>
Pressure Blasting Model	MEC 9182

Flame spraying was preferred due to the reasons that coating can be achieved on large & complex areas (structures), the surface coatings produced are porous and lubricants can be absorbed into the coating, enhancing absorption performance of the target by keeping the composites microstructures remains unaltered [13] as shown by the SEM micrographs of powders and coated samples Fig. 4 and Fig. 5.

In order to enhance the mechanical adhesion of the coating to substrate, they were grit blasted [16-17] by alumina grit with parameters as listed in Table 2.



**Fig. 2 : experimental flame spray at MEC Jodhpur**

The 7075, substrate samples were coated using flame spray by Metallizing Equipment Co. Pvt. Ltd., Jodhpur, India Fig. 2 with the parameters as listed in Table 3. The grit blasted and coated samples are shown in Fig. 3.

**Table 3 : Flame Spray Parameter Details**

Process	Flame Spray
Gun	MEC6P Powder Jet
Coating Thickness	Average 100-150 $\mu$ m
Dye Acetylene Pressure	1-1.1 Kg/cm <sup>2</sup>
Dye Acetylene Flow	55 scfh
Angle of coating	90 <sup>o</sup>
Oxygen Pressure	2Kg/cm <sup>2</sup>
Oxygen Flow	45 scfh
Working Distance	5-6"
Flame Temperature	2000-25000C

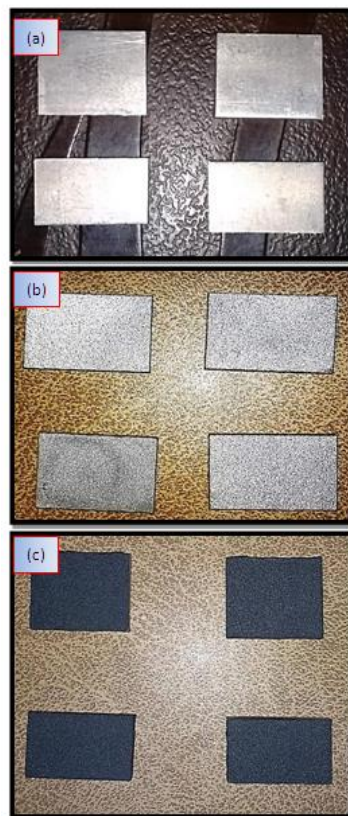


**Fig. 3: substrate samples; (a) samples cut from sheet of Al. Alloy 7075, (b) grit blasted samples, (c) flame sprayed samples**

### 2.3 CHARACTERIZATION

Particle morphology of Al<sub>2</sub>O<sub>3</sub>:TiO<sub>2</sub> with composition 87:13 and 50:50 powders as well as coated samples were performed by scanned electron microscopy [8] using SEM, ZEISS, SUPRA 55. The reflection loss of EM waves was measured using Keysight E-8363C, Vector-Network-Analyzer in X-Band using WR-90 [14-15].

### 3. RESULTS AND DISCUSSIONS

#### 3.1 MORPHOLOGY

Fig. 5 shows the SEM microstructures of sample 1 and sample.

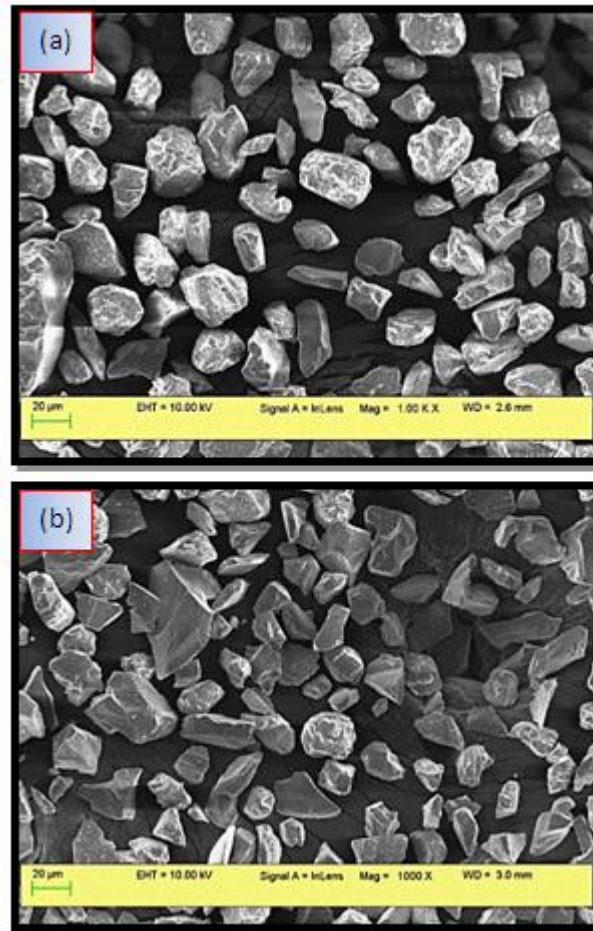


**Fig. 4: powder sem images of Al<sub>2</sub>O<sub>3</sub>: TiO<sub>2</sub> with composition (a) 87:13 and (b) 50:50**

Morphologies of Al<sub>2</sub>O<sub>3</sub>:TiO<sub>2</sub>, in 87:13 and 50:50 commercially available composite powders are shown in Fig. 4, consequently first composition had morphology of dense solid particles with particle size in a range of 15–45  $\mu\text{m}$  and mean particle size of 30  $\mu\text{m}$  whereas the dense solid particles with particle size in a range of 15–43  $\mu\text{m}$  with mean particle size of 32  $\mu\text{m}$  specified by second composition.

Nanocomposite powders showed normal size distributions and presence of small particles of TiO<sub>2</sub> on the surface of Al<sub>2</sub>O<sub>3</sub> particles. The micro structured powders contained agglomerates of small particles.

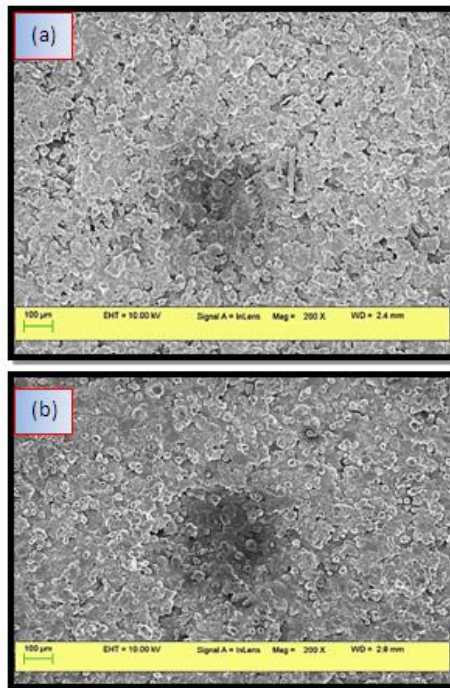


**Fig. 5: sem images of coated al<sub>2</sub>o<sub>3</sub>: tio<sub>2</sub> (a) 87:13 (b) 50:50**

Fig. 4(a) revealed more TiO<sub>2</sub> particle collection on Al<sub>2</sub>O<sub>3</sub> as compared to Fig. 4 (b) due to less proportionate composition of TiO<sub>2</sub> in it. Surface morphologies of the coated samples 1 and sample 2 using flame spraying shown the presence of agglomerate like particles indicated by Fig. 5(a) and 5(b).

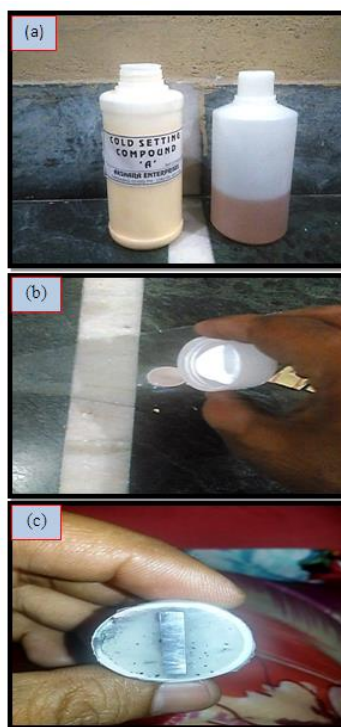


**Fig.6: sample mounting process for cross sectional sem**

Although there is no such significant differences in these two SEM images except that the composites are more agglomerated in Sample 1 than Sample 2. To investigate the cross sectional morphology sample mounting has been done using cold setting compound and cold resin as shown by subsequent Fig. 6(a) and 6(b) followed by polishing of the surface with successive grade emery papers and velvet clothing using rotating wheel technique at DAV University, Jalandhar, Fig. 6(c). The mounted samples were then exposed to scanned electron microscope for cross sectional images of the samples as shown by Fig. 7.



**Fig. 7: sem cross sectional of ceramic coated samples in ratios (a) 87:13 (b) 50:50**

### 3.2 ELECTRICAL PROPERTIES

The microwave absorption property of material is typically characterized in terms of the power reflection of a plane wave reflected from an metallic surface, aluminum alloy 7075 coated by ceramic by flame spraying.

The power reflection or reflectivity of the coating, [3] generally produced for normal incidence, is commonly expressed as:

$$R = 20 \lg|\Gamma| = 20 \lg \left| \frac{Z_{in} - Z_0}{Z_{in} + Z_0} \right| \quad (4)$$

Where,  $\Gamma$ ,  $Z_{in}$  and  $Z_0$  present the reflection coefficient, input impedance of the coating, and intrinsic impedance of free space with a value of  $377 \Omega$  respectively. According to the transmission theory, for a single-layer absorber backed by a perfect conductor, the input impedance of the absorber  $Z_{in}$  of a metal-backed microwave absorbing coating is given:

$$Z_{in} = \eta \tanh(\gamma d) \quad (5)$$

$$\text{Where, } \eta = Z_0 \sqrt{\mu/\epsilon}$$

$$\text{and } \gamma = j \frac{2\pi f}{c} \sqrt{\mu\epsilon}$$

$\eta$ ,  $\gamma$ ,  $d$ ,  $\epsilon$  and  $\mu$  denote the intrinsic impedance, propagation constant, thickness, relative complex permittivity and permeability of the composite coating respectively.  $c$  and  $f$  are the velocity of light and the frequency of wave incident. As we know, in order to design microwave absorbing coating with a high performance, two important conditions should be satisfied [18]. The first condition is impedance matching, which requests the input impedance of coatings should be made approximate to the impedance of free space insuring the microwave enters absorption coatings as much as possible. When  $Z_{in} = Z_0$ , the impedance matching is satisfied perfectly, and EM wave will be incident completely without any reflection, theoretically. Secondly, the incident wave should be attenuated rapidly through the material layer as far as possible.

In order to characterize the microwave absorbing properties of the composite coatings based on Al alloy sheet, the reflection loss (RL) curves versus frequency for different compositions of ceramics oxides are shown in Fig. 8. The composition, in weight ratios 87:13 and 50:50 has been studied. The sweeping frequency was ranged from 8 to 12 GHz (X-Band).



**Fig. 8: electrical testing for reflection loss calculation,  $S_{11}$**

At microwave frequencies, various measurement techniques like free space measurement technique, resonant cavity technique, transmission line technique, dielectric probe technique are available. In this work, dielectric probe technique is used to measure  $S_{11}$  parameters. It includes a 50GHz Agilent network analyzer having Agilent Technologies 85071 measurement software. Before Measurement, Calibration of VNA is required. There are 2 steps for measurement of S parameters.

### 3.2.1 CALIBRATION PHASE

The process of calibration is also called as Vector Error Correction. Vector-error correction is the process of characterizing systematic error terms by measuring known calibration standards, and then removing the effects of these errors from subsequent measurements. Before measuring, calibration at the tip of the probe must be performed. It corrects for the directivity, tracking, and source match errors that can be present in a reflection measurement. The Method used for the calibration before measurement of dielectric constant is called one port calibration method. Calibration is done with standard calibration kit provided with the VNA and originally calibrated results are stored in a file in the VNA named as calibration kit. The empty WR 90 Waveguide is inserted between the two port co-axial cables of VNA and then the dielectric constant of air is made to real at value 1.

### 3.2.2 CALCULATION PHASE

After calibration of VNA, coated samples are carefully placed under the surface of WR-90 in a manner that it

properly covers the openings of WR90. The measurement was done in the range of 8GHz – 12GHz with WR-90 wave guide.

The measured S11 parameter at various frequency points in the range 8.2GHz to 12.4GHz from VNA was plotted using MATLAB as shown in Fig. 9. It is found that the allowable reflection loss ( $RL \leq -10$  dB, for over 90% microwave absorption) can get in the frequency range of 9.238GHz – 10.2GHz by varying the composition of coating composites. It is worth noting that, in Fig. 9(a), the sample 1 display good absorption properties over  $>4$ dB in the complete X band and exhibits  $>90\%$  absorption properties from 9.238GHz – 10.2GHz and extreme reflection loss of -13.6dB at 9.683GHz. Whereas by increasing the content of TiO<sub>2</sub> i.e. sample 2 with 50:50 % composition of Al<sub>2</sub>O<sub>3</sub>:TiO<sub>2</sub>,  $<-10$ dB absorption was monitored from 9.28GHz to 9.82GHz with maximum reflection loss of -11.936dB at 9.53 GHz. Hence it is experimentally being concluded that 87:13 composition of Al<sub>2</sub>O<sub>3</sub>:TiO<sub>2</sub> ceramics gives better absorption at broader band width than 50-50 composition as shown by S11 characteristics of both the samples plotted simultaneously in Fig. 9(c).

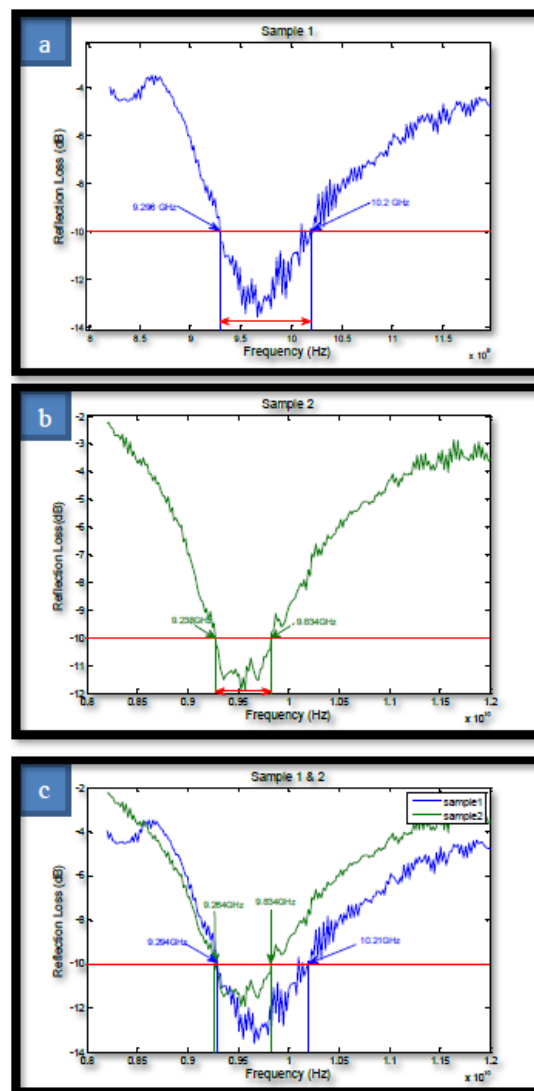


**Fig. 9: the reflection-loss spectra S<sub>11</sub>: (a) sample 1 (b) sample 2 (c) combined sample 1 & 2**

#### 4. CONCLUSION

The fabrication of Al<sub>2</sub>O<sub>3</sub> : TiO<sub>2</sub> ; two different compositions as 87:13 and 50:50 coatings with flame spraying was studied and experimentally tested using VNA in X band. It was found that Flame Spraying preserves the shape due to less temperature operation involved in the process results in production of effective radar absorbing coatings and exhibits more than 90% absorption. It is concluded that 87:13 composition of Al<sub>2</sub>O<sub>3</sub> : TiO<sub>2</sub> results in better reflection loss of -13.6dB in the frequency range 9.238GHz – 10.2GHz than 50:50 composition as it results in maximum reflection loss of -11.936dB from 9.28GHz to 9.82GHz.

#### REFERENCES

- [1] Vinoy, K.J., Jha, R.M, Radar Absorbing Materials From Theory to Design and Characterization, Springer US , 978-1-4613-8065-8
- [2] <http://www.thermalspray.org/>
- [3] Duan Yupinga, Wu Guanglia, Gu Shuchao, Li Shuqing, Ma Guojiab, Study on microwave absorbing properties of carbonyl-iron composite coating based on PVC and Al sheet, Applied Surface Science 258 (2012) 5746– 5752.
- [4] Chang-feng Zhang, Wen Tang, Xiao-Iong Mi, Le-ran Chen, Application of Radar Absorbing Material in Design of Metal Space Frame Radomes, 2011 Cross Strait Quad-Regional Radio Science and Wireless Technology Conference 222-225.
- [5] Ganesan, L. J. (2013). Reduction of Electromagnetic Interference in Three Phase Squirrel Cage Induction Motor by Coating of Nano Composite Filled Enamel to the Windings of the Motor, 978–981.
- [6] Suneet Gupta , Gagan Deep, Agricultural Waste Based-Coco Peat And Coconut Shell Activated Carbon Microwave Absorber, Proceedings of , International Microwave and RF Conference 2016, 978-1-5090-4685-0/16 ©2016 IEEE.
- [7] Yang, Z., Luo, F., Zhou, W., Zhu, D., & Huang, Z. (2016). Design of a broadband electromagnetic absorbers based on TiO<sub>2</sub>/Al<sub>2</sub>O<sub>3</sub> ceramic coatings with metamaterial surfaces. Journal of Alloys and Compounds, 687, 384–388. <https://doi.org/10.1016/j.jallcom.2016.06.166>
- [8] Dejang, N., Watcharapasorn, A., Wirojupatump, S., Niranatlumpong, P., & Jiansirisomboon, S. (2010). Fabrication and properties of plasma-sprayed Al<sub>2</sub>O<sub>3</sub>/TiO<sub>2</sub> composite coatings: A role of nano-sized TiO<sub>2</sub> addition. Surface and Coatings Technology, 204(9–10), 1651–1657. <https://doi.org/10.1016/j.surfcoat.2009.10.052>
- [9] Merati, A. (2011). Materials Replacement for Aging Aircraft. Corrosion Fatigue and Environmentally Assisted Cracking in Aging Military Vehicles, (Mmc), 22. Retrieved from <ftp://ftp.rta.nato.int/PubFullText/RTO/AG/RTO-AG-AVT-140///AG-AVT-140-24.pdf>
- [10] Lin, C. T., Swanson, B., Kolody, M., Sizemore, C., & Bahns, J. (2003). Nanograin magnetoresistive manganite coatings for EMI shielding against directed energy pulses. Progress in Organic Coatings, 47(3–4), 190–197. [https://doi.org/10.1016/S0300-9440\(03\)00138-3](https://doi.org/10.1016/S0300-9440(03)00138-3)

- [11] Bhattacharya, P., Sahoo, S., & Das, C. K. (2012). Microwave absorption behaviour of MWCNT based nanocomposites in X-band region. *Express Polymer Letters*, 7(3), 212–223. <https://doi.org/10.3144/expresspolymlett.2013.20>
- [12] Duggal, S., Aul, G. D., & Chawla, V. (2017). Investigation of absorption properties of Sugarcane Bagasse-Coal pyramidal microwave absorber. In *Asia-Pacific Microwave Conference Proceedings, APMC*. <https://doi.org/10.1109/APMC.2016.7931361>
- [13] Lisjak, D., Lintunen, P., Hujanen, A., Varis, T., Bolelli, G., Lusvarghi, L., ... Drofenik, M. (2011). Hexaferrite/polyethylene Composite coatings prepared with flame spraying. *Materials Letters*, 65(3), 534–536. <https://doi.org/10.1016/j.matlet.2010.10.076>
- [14] Kaur, R., Aul, G. D., & Chawla, V. (2015). Improved reflection loss performance of dried banana leaves pyramidal microwave absorbers by coal for application in anechoic chambers. *Progress In Electromagnetics Research M*, 43.
- [15] Kaur, H., Deep, G., & Chawla, V. (2015). Enhanced Reflection Loss Performance of Square Based Pyramidal Microwave Absorber Using Rice Husk-Coal, 43(September), 165–173.
- [16] Espallargas, N. (2015). *Thermal Spray Coatings*, 5(65), 497–509.
- [17] Matikainen, V., Niemi, K., Koivuluoto, H., & Vuoristo, P. (2014). Abrasion, Erosion and Cavitation Erosion Wear Properties of Thermally Sprayed Alumina Based Coatings. *Coatings*, 4(1), 18–36.
- [18] Yuping, D., Guangli, W., Shuchao, G., Shuqing, L., & Guojia, M. (2012). Study on microwave absorbing properties of carbonyl-iron composite coating based on PVC and Al sheet. *Applied Surface Science*, 258(15), 5746–5752.